Mansoura Engineering Journal

Volume 14 | Issue 1 Article 12

5-24-2021

Numerical Solution of Magnetostatic Field in and around Current Carrying windings of Electrical Machines.

S. Elorieny
Electrical Power Engineering Department, Faculty of Engineering, Mansoura University, Mansoura, Egypt.

M. El-Shamoty
Electrical Power Engineering Department, Faculty of Engineering, Mansoura University, Mansoura, Egypt.

A. Amin
Electrical Power Engineering Department, Faculty of Engineering, Mansoura University, Mansoura, Egypt.

Mansoura Engineering Journal ,MEJ, Vol. 14 , No. 1 , June 1989 E. 7

NUMERICAL SOLUTION OF MAGNETOSTATIC FIELD IN AND AROUND CURRENT CARRYING WINDINGS OF ELECTRICAL MACHINES

الحل الرقمى للمجال المغناطيسى الاستاتيكى داخل وحول منطقة الموصلات الكهربية فى الآت الكهربية

S. A. ELDRIENY M. M. Y. EL-SHAMOTY A. R. A. AMIN
Electrical Engineering Department , Faculty of Engineering,
El-Mansoura University , El-Mansoura , E G Y P T

الخلاصة – نظرا لان مركبة المجال المغناطيسى الاستاتيكى داخل أو حول منطقة الموصلات الكهربية فى الآت الكهربية الناشئة لهذا المجال صغيره الاتجاه لذلك عد حساب توزيع كثافة الفيض المغناطيسى فى هذه المنطقة فان معادلة لابلاس المشتقة من المعادلات التفاضلية الجزئية للمجال فى ثلاثة اتجاهات لا تمثل المركبات المجال المتعبرة الاتجاه وبالتالى فان مجموعة المعادلات التفاضلية المحدده يلزم لها بعض التعديلات حتى تمثل مركبات المجال المغناطيسى الاستاتيكى داخل أو حول منطقة الموصلات الكهربية . فى هذا البحث تم ادخال والاخذ فى الاعتبار مصادر للفيض عند سطحى منطقه نهايات الملفات وقسمة هذه المصادر نصاب الى القيمة المتغيرة عند حساب قيمة الجهد المغناطيسى الاستاتيكى فى هذه المناطق ومن ثم أمكننا بهذا التعديل الحصول فى نتائج نظرية أقرب الى النتائج العمليه منها لو أهملنا هذه المصادر عند الحساب بطريقة المعادلات التفاضلية المحددة .

ARSTRACT :

An accurate knowledge of magnetostatics as well as other field distribution in electrical machines is of great importance in design optimization. The search activity in the past two decades has considered the numerical analysis and calculation of magnetostatic field in electrical machinery through the solution of Maxwell's equations , while taking full account of magnetic saturation. This solution of field problem is limited to simple geometric shapes of the region of interest. Concepts of both scalar and vector magnetic potential have been used for computing the magnetostatic fields. Numerical approaches involving finite-element method , finite-difference method and integral equation technique may he used to evaluate such fields.

In electrical machines , the flux distribution required is that in and around current carrying windings. Consequently the partial differential equation such as Laplace's equation for the behaviour of magnetostatic fields is not valid within current carrying conductors. Within the conductor there is no defintion in the finite-difference mesh. It is however possible to derive another potential function inside the current-carrying regions which do not satisfy Laplace's equation

throughout the conductor , but enable the field problem to be solved and allow calculation of magnetic field strength and flux density. These equations affect a solution of Poission's equation which does hold inside a current-carrying region but only for vector magnetic potentials.

This paper presents the development of finite-difference method for solving three-dimentional scalar magnetostatic potential in and around current-carrying windings in electrical machines. Consequently, an appropriate field sources and the armature current distribution in slotted sections and overhang regions are easy derived.

1. INTRODUCTION :

The fluxes in the end regions of electrical machine are generated by windings whose end-connections are of complex shape, and these generate a three-dimensional flux pattern whose computation is of increasing importance in linear machines and similar cases . The winding forces can satisfactory be predicted by numerical integration over the current elements, but this is not well suited to the problem of field prediction in and around the surrounding materials. Differential methods are then more convenient , preferably in terms of a scalar function since the magnetic vector potential has three components. In practic, the complexity of the end winding and the need to specify three components of the current density vector makes it difficult to provide a suitably simplified model to describe the end-winding , and hence the scalar potential field sources which are derived from it.

For many purprises, it is convenient to compute the fields in terms of travelling waves. The computation of the sources of each wave component ,in numerical terms, demands firstly ; a simple description of the current distribution in the region of current carring winding , such as slotted sections and the over hang region , secondly ; an insight into the various ways which it can be transformed.

The paper presents a development of finite difference method for solving three dimensional scalar magnetostatic potential in and arround current carrying windings. This development examines the general problems of translating complex current distribution into equivelent nodal sources for a numerical scalar potential computation by finite difference method. The method is applied to linear synchronous machine end region and illustrated by field solution.

2. THE BASIC ANALOGUE OF SINGLE NODE :

The FDM places the nodes at the corner of cubes , the cube has 1 cm length. Each of the six elements connected to a node is taken to have

unit permeance unless an iron boundary is less than 1 cm distance when the reluctance is proportionaly small. Thus, in Fig.1 , the node potential is given by:

$$P_1 + P_2 + P_3 + P_4 + P_5 + P_6 - 6P_0 = 0 \qquad (1)$$

Where p is the magnetic scalar potential difference between different points and denotes the magnetomotive force which excits between these points. In the case of a half pole pitch region in an electrical machine , the three dimensional mesh is likely to have several thousands of branches,therefore it is solved by representing it in a computer and applying a technique known as successive over relaxation (SOR). Relaxation of a network consists of treating all nodes in sequence of one node at a time. If the left hand side of the above equation is evaluated for an arbitrary choise of node potentials, a quantity not equal to zero will most likely result. This is called residual and is proprtional to the total flux converting on the central node. The residual at all nodes should for successive iteration (one calculation per node for all nodes) be very small compared with flux passing through any one element (they should ideally be zero). If the potential P_0 is adjusted after each iteration the residual for the node can be reduced to zero. By treating nodes one a time, many times over,the successive adjustments cause the residuals to gradually diffuse around the mesh to be absorbed by the boundaries of a constant potential. This is called successive relaxtion. Now the residual R is given by :

$$R = P_1 + P_2 + P_3 + P_4 + P_5 + P_6 - 6P_0 \qquad (2)$$

Adding a quantity of R/6 may reduce the residual to zero. Adding a quantity $\alpha R/6$, if α is greater than one , causes a greater change.Where α affects the convergence of the solution. Higher values of α improve the rate of convergence, but if too large a value is used instability and oscillation may result , thereby preventing convergence may be obtained [5].

3. CURRENT DISTRIBUTION :

A useful method is described by Carpenter [4] where the electric circuits (the current carrying region) and the magnetic circuits (the complete filed including the space inside the conductor) are initially torn apart. This is illustrated for a rectangular conductor (Fig 2a) as follows.

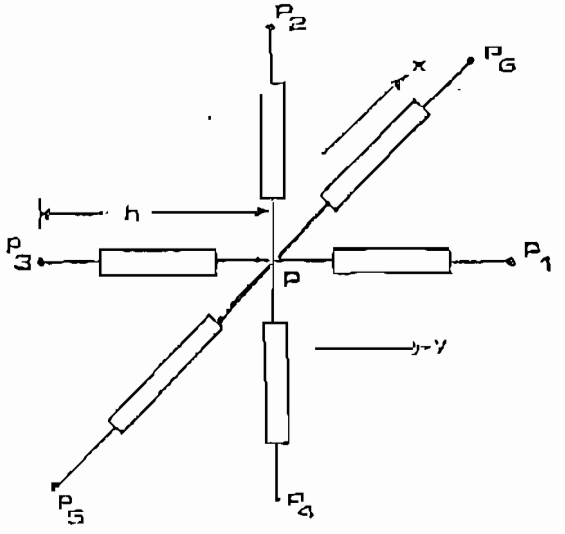

Fig.(1): Electrical analogue of a single node.

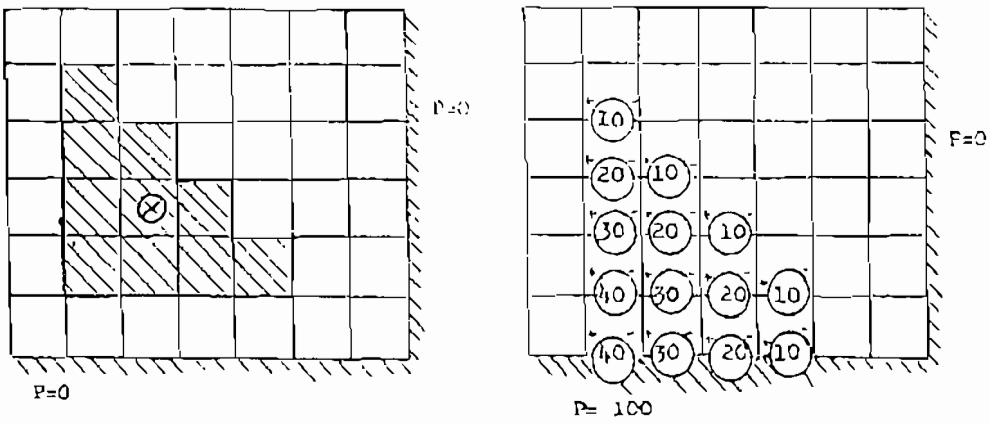

Fig.(2a) : Current carrying region (J=10 Amps./square).

Fig.(2b) : Branch M.M.F. source inserted after tearing the conductor out of the mesh.

(a) The conductor is torn from the mesh circut analogue in the downward direction.
(b) Branch sources of potential are inserted, which have been broken in the tearing process , equal to the ampere conductor which have passed through the branch. The path of withdrawn of any conductor is arbitrary , see Fig.2b.
(c) The branch sources are converted to their Norton equivalents (Fig 3a and 3b). The flux source values are simply added to the residual calculated at the node during relaxation. The conductor has collapsed to from a current sheet on the iron surface and the branch sources have been retained to define the fixed potentials.
(d) The relaxation process is then executed resulting in a non-zero divergence field solution. (The solution is valid everywhere except within the original conductor section).
(e) The introduction of flux sources obviously created a field of non-zero divergence. The potential function now defined within the conductor represents a field which is grossly distorted.
The field outside the region converted by flux sources is correctly defined by the normal magnetostatic potential function but within the conductor, corrective fields of opposite divergence must be added to those calculated from the function. This complementary field is defined by branch sources as shown in Fig 4. This method was used simply to represent the field and armature windings. In the case of the latter the winding is simplified to a thick current sheet with components in axial (x) and transverse (y) directions. The currents are assumed to be uniformly distributed in the (z) direction for depth of the winding. It is not possible to define separate current distributions for the top and bottom layers of the winding without both destroying the symmetry and the need for a mesh of twice the size. The winding is withdrawn from the mesh by collapsing the end turns (over-hang) into the sides of the centre limb (Fig 5a,5b) thus forming current sheets along the slot ends rather like the end rings of a squirrel cage rotor. Flux sources appear on the upper and lower surface of the winding. The complementary field is applied between the two layers of flux sources and has a component in the Z direction only. The magnitudes of flux source are derived as follows:

3.1. Magneto Motive Force in Slotted Sections :

The armature winding is represented by a thick current sheet, assuming that current is uniformly distributed in the (z) direction. If the winding has short chorded coils of pitch C_p , the displacement between the two peaks of current loading in the top layer and bottom

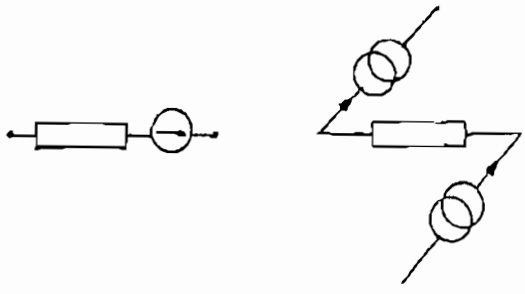

Fig.(3a) : Norton equivalent of branch source.

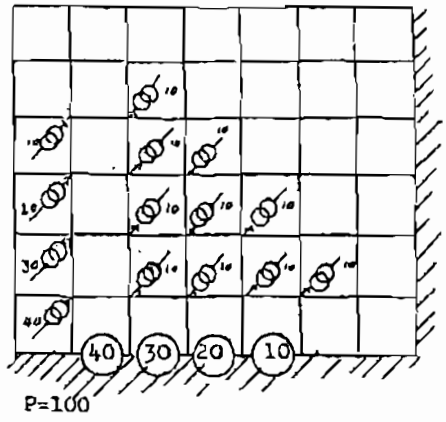

Fig.(3b) : Branch sources replaced by equivalent model sources.

Fig.(4) : The complementary field having opposite divergence.

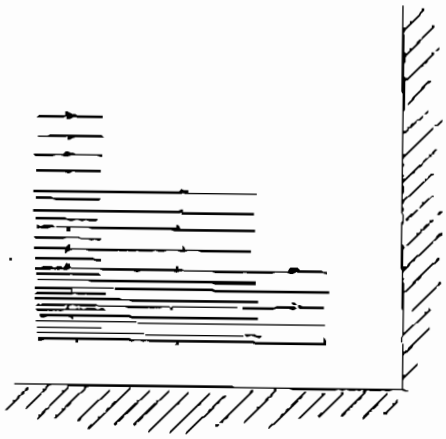

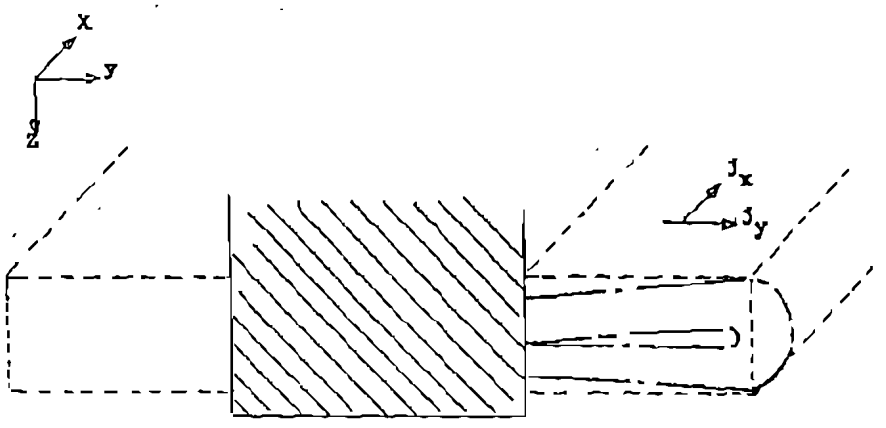

Fig.(5a) : Armature winding as a thick current sheet.

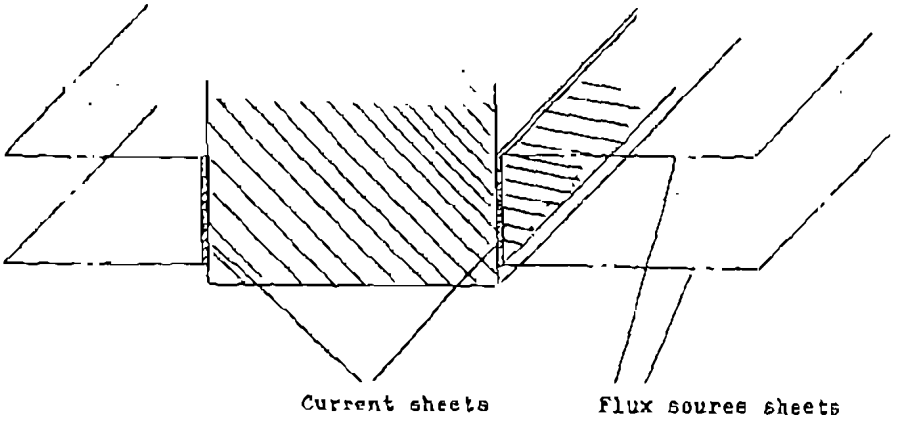

Fig.(5b) : End turns collapsed to form current sheets and nodals flux sources inserted.

layer windings will be :

$$\delta = \pi \left(1 - (C_p/p) \right) \tag{3}$$

Where C_p is coil pitch , p is pole pitch.

If the peak current loading is $\hat{J}_D$, then the current distribution in the slotted region is made up of two components:

(i) due to upper slot conductors ;

$$J_{s1}(x) = \frac{\hat{J}_D}{2} \cdot \cos\left(\frac{\pi x}{p} - \frac{\delta}{2}\right) \tag{4}$$

(ii) due to lower slot conductors ;

$$J_{s2}(x) = \frac{\hat{J}_D}{2} \cdot \cos\left(\frac{\pi x}{p} + \frac{\delta}{2}\right) \tag{5}$$

The total current loading is the sum of the previous two components and is given by ;

$$J_s(x) = \hat{J}_D \cdot \cos\frac{\delta}{2} \cdot \cos\frac{\pi x}{p} \tag{6}$$

Hence, the magneto motive force ,m.m.f., of the slotted section is given by ;

$$F_s(x) = \int J_s(x).dx$$

$$F_s(x) = \hat{J}_D \cdot \cos\frac{\delta}{2} \int \cos\frac{\pi x}{p}.dx$$

$$= \frac{\hat{J}_D p}{\pi} \cos\frac{\delta}{2} \sin\frac{\pi x}{p} \tag{7}$$

Assuming,

$$\hat{J}_D \cdot p/\pi = 100 \quad \text{units}$$

For the direct axis armature field with its peak m.m.f. coincides with the pole centre (x = 1) and varying sinusoidally to zero m.m.f. at the half pole pitch mesh (x=p/2 + 1) . The FDM solution represented over a quarter of a full m.m.f. wave. For the direct axis, the m.m.f. equation is ;

$$F_s(x) = 100 \cdot \cos\frac{\delta}{2} \cdot \sin\frac{\pi}{p}\left(\left(\frac{p}{2}+1\right)-x\right) \tag{8}$$

For quadrature axis field, with zero m.m.f., corresponding to the pole centre (x = 1) and varying sinusoidally to a peak m.m.f. at the half pole pitch (x = p/2 + 1), the m.m.f. equation is :

$$F_s(x) = 100 \cdot \cos\frac{\delta}{2} \cdot \sin\frac{\pi}{p}(x-1) \qquad (9)$$

3.2. Magneto Motive Force in Overhang Section :

In the overhang the top layer conductors will be angled forwards (+ve x direction) and the bottom layer conductor will be angled backwards with respect to the axis (x) of the stator .
At a point p(x,y) in the overhang (see Fig 6a) the top layer produces the following currents.

$$J_y = J_{s1}(x - a) \qquad (10)$$

$$J_x = J_{s1}(x - a)\cot\theta \qquad (11)$$

and the bottom layer will contribute;

$$J_y = J_{s2}(x + a) \qquad (12)$$

$$J_x = J_{s2}(x + a)\cot\theta \qquad (13)$$

Where , $\cot\theta = C_p/2w_a$ and w_a is the overhang length .

$$a = y\cot\theta = y.C_p/2w_a$$

The current distributions are therefore:

$$J_y(x,y) = \frac{\hat{J}_o}{2}\cos\left(\frac{\pi x}{p} - \frac{\delta}{2} - \frac{\pi y C_p}{2w_a p}\right) + \frac{\hat{J}_o}{2}\cos\left(\frac{\pi x}{p} + \frac{\delta}{2} + \frac{\pi y C_p}{2w_a p}\right) \qquad (14)$$

$$J_x(x,y) = \frac{\hat{J}_o C_p}{4\omega_a}\cos\left(\frac{\pi x}{p} - \frac{\delta}{2} - \frac{\pi y C_p}{2\omega_a p}\right) - \frac{\hat{J}_o C_p}{4\omega_a}\cos\left(\frac{\pi x}{p} + \frac{\delta}{2} + \frac{\pi y C_p}{2\omega_a p}\right) \quad (15)$$

$$J_y(x,y) = \hat{J}_o \cos\left(\frac{\delta}{2} + \frac{\pi y C_p}{2\omega_a p}\right)\cos\frac{\pi x}{p} \quad (16)$$

$$J_x(x,y) = \frac{\hat{J}_o C_p}{2\omega_a}\sin\left(\frac{\delta}{2} + \frac{\pi y C_p}{2\omega_a p}\right)\sin\frac{\pi x}{p} \quad (17)$$

These expressions may be checked by calculating div J and equating it to zero.

$$\text{div } J = \frac{\partial J_x(x,y)}{\partial x} + \frac{\partial J_y(x,y)}{\partial y}$$

$$\frac{\partial J_x(x,y)}{\partial x} = \frac{\hat{J}_o C_p}{2\omega_a} \cdot \frac{\pi}{p} \cdot \sin\left(\frac{\delta}{2} + \frac{\pi y C_p}{2\omega_a p}\right) \cdot \cos(\pi x/p)$$

$$\frac{\partial J_y(x,y)}{\partial x} = -\frac{\hat{J}_o C_p}{2\omega_a} \cdot \frac{\pi}{p} \cdot \sin\left(\frac{\delta}{2} + \frac{\pi y C_p}{2\omega_a p}\right) \cdot \cos(\pi x/p)$$

Hence, $$\frac{\partial J_x(x,y)}{\partial x} + \frac{\partial J_y(x,y)}{\partial y} = 0$$

Hence, div J = 0 , satisfied.

If, as shown in Fig.6b. the overhang is collapsed to form a thin sheet on the sides of the core, the branch potential source which must appear along AB, must be equal to the ampere turns which have cut the line AB.

$$F_o(x,y) = \int_y^{w_a} J_x(x,y)\,.dy = \frac{\hat{J}_o C_p}{2w_a}\sin\frac{\pi x}{p}\int_y^{w_a}\sin\left(\frac{\delta}{2} + \frac{\pi y C_p}{2w_a p}\right).dy$$

$$= \frac{\hat{J}_o C_p}{\pi}\sin\frac{\pi x}{p}\left[\cos\left(\frac{\delta}{2} + \frac{\pi y C_p}{2w_a p}\right) - \cos\left(\frac{\delta}{2} + \frac{C_p \pi}{2p}\right)\right]$$

since $\delta = \pi(1 - C_p/p)$ the last term is zero, hence the m.m.f. in the

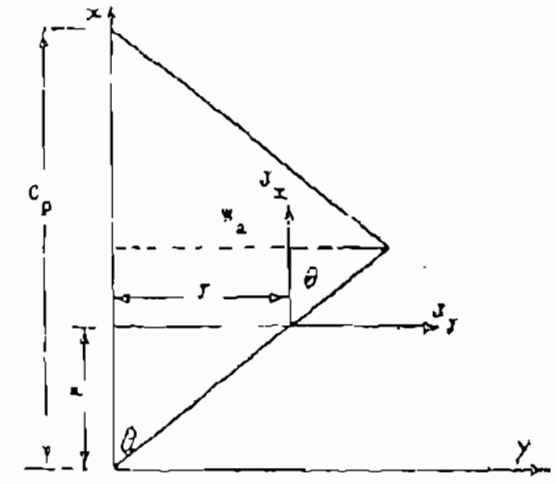

(a)

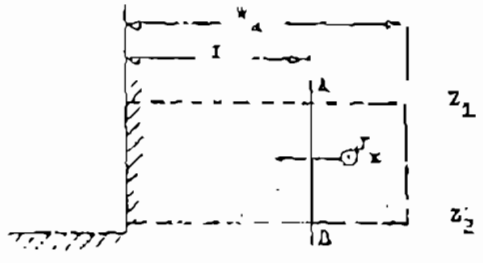

(b)

Fig.(6) : Overhang collapsed to form a thin current sheet on both sides of the core and nodals flux sources appeared on the planes z_1 and z_2 .

overhang section is given by :

$$F_o(x,y) = \frac{\hat{J}_\sigma \rho}{n} \cos\left(\frac{\delta}{2} + \frac{n y C_\rho}{2 w_a \rho}\right) \sin\frac{n x}{\rho} \qquad (18)$$

If substituted by equation (7) into Eq.(18), hence :

$$F_o(x,y) = \frac{F_s(x)}{\cos\frac{\delta}{2}} \cos\left(\frac{\delta}{2} + \frac{n y C_\rho}{2 w_a \rho}\right) \quad , 0 < y < w_a \qquad (19)$$

if $y=0$ then $F_o(x,y) = F_s(x)$
if $y=w_a$ then $F_o(x,y) = 0$
The nodal flux sources appearing on the surface planes are :

$$F_o(x,y)/(z_2 - z_1) \quad \text{for plane } z_2 \qquad (20)$$

$$-F_o(x,y)/(z_2 - z_1) \quad \text{for plane } z_1 \qquad (21)$$

For the part of the armature winding between the core and the first bend, flux sources using the potential $F_s(x)$ are used.

4. APPLICATION AND COMPARISON WITH THE EXPERIMENTAL RESULTS :

The method is elaborated in this paper and illustrated by translating complex current distribution of the over-hang sections into equivalent nodal flux sources appearing on the upper and lower surface of the winding in the over-hang region. The complementary field is applied between the two layer of flux sources and has a component only in the direction perpendicular to the plane containing the over-hang winding (Z-direction). This method is applied easy to linear synchronous machine over-hang and illustrated by field solutions. The stator armature windings are composed of a number of continuously distributed and uniformly spread coils which span 2/3 of the pole pitch.
The computation of the field due to A.C. windings was carried out assuming sinusoidal distribution of both armature current and M.M.F.. In relation to the track poles the windings M.M.F. was regarded as comprising a direct-axis and quadrature axis sinusoidally distributed component.

(a) The armature direct-axis field :

The direct-axis field has the same symmetry as the magnetizing field and few changes to the computations were required. The side limbs are set at zero potential , while along the centre limb the potential is set to vary sinusoidally. The peak of the M.M.F. wave (an arbitrary refrence of 100 units) coincides with the pole centre and the mesh covers one quarter of a length. The equation of M.M.F. distribution at the armature surface is:

$$100 \cos\left(\frac{\pi}{pp}(x-1)\right)$$

and x varies from x = 1 at the pole centre to x = pp/2 +1

(b) The armature quadrature axis field :

The quadrature axis field has a different symmetry since the track-pole axis coincides with the zero point of the armature M.M.F. wave. This means that the pole and Y-Z plane passing through the pole centre must also be at zero potential. The field becomes almost entirely axial since the pole and both side limbs are at zero potential. The distribution of M.M.F. at the armature surface is given by:

$$100 \sin\left(\frac{\pi}{pp}(x-1)\right)$$

and x varies from x=1 at the pole centre to pp/2 + 1.

The mesh covers one quarter of wave length. The compensation of the overhang turns is treated separately as previously explained. The lay-out of 3-dimensions for half pole pitch, Fig.7 , represented the coil and overhang dimensions. The flow-chart, Fig.8 , represents the obtained flux sources due to A.C. windings in the over-hang and slotted sections according to the previously analysis.

Laboratory measurements which are carried on the experimental model, [6] show for good approximation, a resonable agreements with the devolped technique represented in this paper. The following table shows the comparison between the experimental measurements, computed results , and the computed developement FDM of armature flux/pole for 100 AT excitation.

Experimental Measurements	Computed Results With Considering Flux Sources (Developed Technique)	Computed Results Without Considering Flux Sources
3.1×10^{-2} mwb.	3.2×10^{-2} mwb.	3.4×10^{-2} mwb.

Comparison between the experimental measurements and the two computed results of armature flux per pole for 100 AT , 10 mm air gap , and pole depth 20 mm

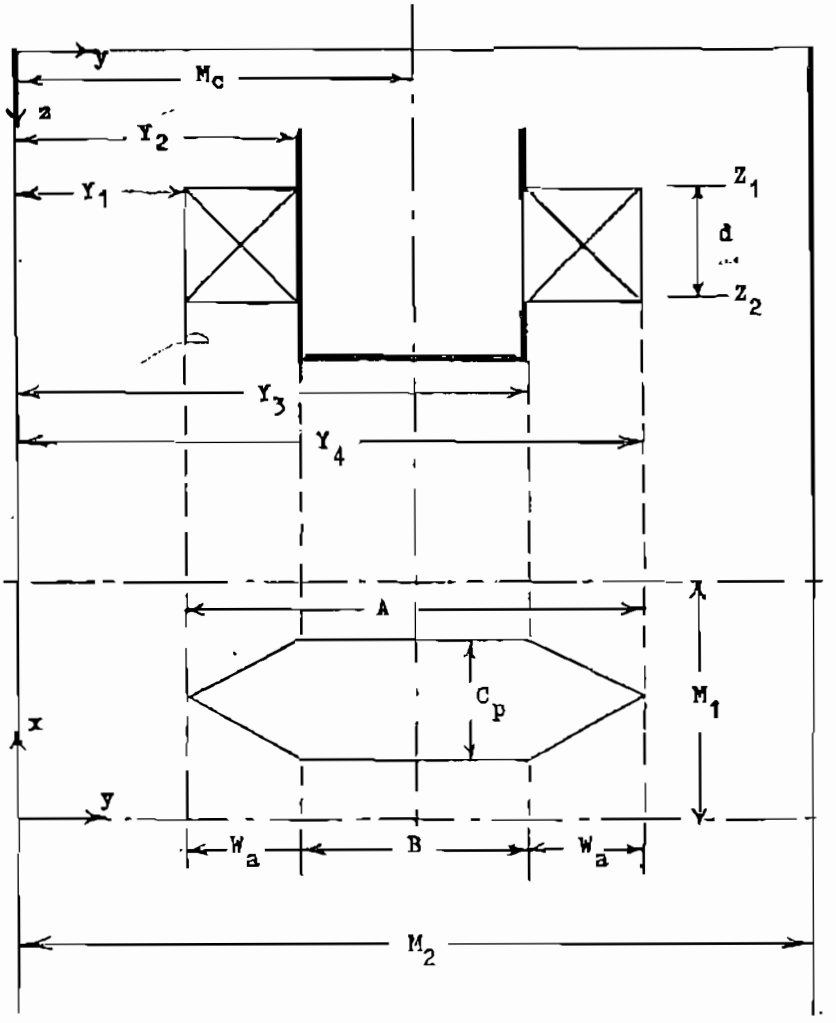

Fig.(7) : Layout of three dimension for half pole-pitch showing the coil and over-hang dimensions.

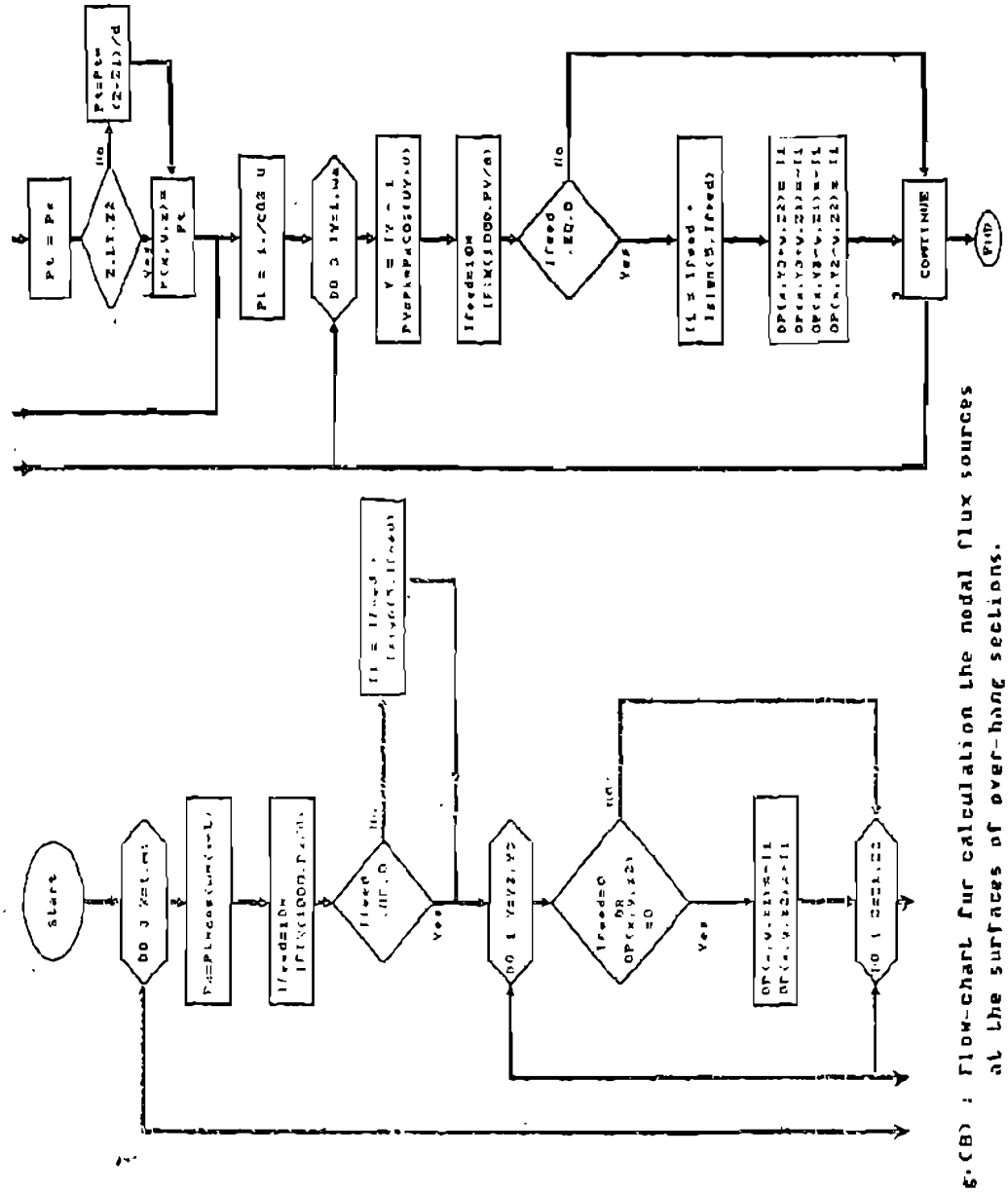

Fig.(B) : Flow-chart for calculation the nodal flux sources at the surfaces of over-hang sections.

5. CONCLUSION :

The finite difference method for solving three dimentional scalar magnetostatic potential in and around current-carrying windings in electrical machines has been developed and presented in this paper.
The armature current distribution and the magnetomotive force M.M.F. in both the over-hang and slotted sections are derived. The approach adopted in this paper has been written in Fortran four computer program and nodal flux sources appearing on the surface planes of the over-hang section are added to the residual during calculation of the nodes potential of these planes. The approach has been applied to a network model represents a static linear synchronous motor excited with one hundred of M.M.F. alternating current. The armature flux per pole has been measured and it has a resonable agreement with the developement of finite difference method FDM.

6. REFERENCES :

1- Binns,K.J. and Lawrenson, P.J., "Analysis and computation of electric and magnetic field problems" , Pergamon Press Ltd., 2nd edition , 1973.

2- Sylvester, P.,"Modern electromagnetic fields" Prentice Hall, 1968.

3- Vitkovitch, D., "Field analysis : experimental and computional methods" , Van Nostrand, 1966.

4- Carpenter, C.J., "Numerical solution of magnetic fields in the vicinity of current-carrying conductors", Proc. I.E.E., Vol. 114, No.11, Nov. 1967.

5- Carpenter, C.J., " Finite-element network models and their application to eddy current problems", Proc. I.E.E., 1975. Vol. 122, pp 455-462.

6- El-Drieny, S.A., " Optimization of track-pole geometry for E-core homopolar linear synchronous motor", Mansoura Engineering Journal , Vol. 12 , No. 2. , Dec. 1987.

LIST OF SYMBOLS :

pi = 3.14159
p := pole pitch = $(M_1 - 1) * 2$
L = 1 , in d-axis M.M.F.
d := depth of the over-hang section
M_c := centre of the model
B := effective coil length
w_a := over hang lenght
$Y_3 = (B + 1)/2 + M_c$
$Y_2 = M_2 - Y_3 + 1$
cp := coil pitch
w = pi/p
L = M_1 , in q-axis M.M.F.
$= z_2 - z_1$
$= (M_2/2 + 1)$
A := total coil length
$= Y_4 - Y_3 = Y_2 - Y_1$
$Y_4 = (A + 1)/2 + M_c$
$Y_1 = M_2 - Y_4 + 1$
δ := displacment between the peaks of current loading = 2V = w.(p-cp)
$U = cp/2 * w/w_a$
$P_k = 100/\cos V$